

Weakly-supervised Video Anomaly Detection with Contrastive Learning of Long and Short-range Temporal Features

Yu Tian^{1,3} Guansong Pang¹ Yuanhong Chen¹ Rajvinder Singh³
 Johan W. Verjans^{1,2,3} Gustavo Carneiro¹

¹ Australian Institute for Machine Learning, University of Adelaide

² Faculty of Health and Medical Sciences, University of Adelaide

³ South Australian Health and Medical Research Institute

Abstract

In this paper, we address the problem of weakly-supervised video anomaly detection, in which given video-level labels for training, we aim to identify in test videos, the snippets containing abnormal events. Although current methods based on multiple instance learning (MIL) show effective detection performance, they ignore important video temporal dependencies. Also, the number of abnormal snippets can vary per anomaly video, which complicates the training process of MIL-based methods because they tend to focus on the most abnormal snippet – this can cause it to mistakenly select a normal snippet instead of an abnormal snippet, and also to fail to select all abnormal snippets available. We propose a novel method, named Multi-scale Temporal Network trained with top- K Contrastive Multiple Instance Learning (MTN-KMIL), to address the issues above. The main contributions of MTN-KMIL are: 1) a novel synthesis of a pyramid of dilated convolutions and a self-attention mechanism, with the former capturing the multi-scale short-range temporal dependencies between snippets and the latter capturing long-range temporal dependencies; and 2) a novel contrastive MIL learning method that enforces large margins between the top- K normal and abnormal video snippets at the feature representation level and anomaly score level, resulting in accurate anomaly discrimination. Extensive experiments show that our method outperforms several state-of-the-art methods by a large margin on three benchmark data sets (ShanghaiTech, UCF-Crime and XD-Violence). Code is available at <https://github.com/tianyu0207/MTN-KMIL>.

1. Introduction

Video anomaly detection has been intensively studied because of its potential to be used in autonomous surveillance systems [14, 51, 59, 70]. The goal of video anomaly

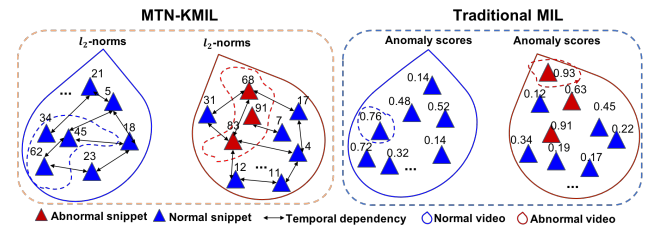


Figure 1. The proposed MTN-KMIL with $K = 3$ (left) vs. MIL that aims to select the most abnormal snippet (right) for weakly supervised video anomaly detection, where anomaly videos may contain a variable number of abnormal snippets. MTN-KMIL explores long and short-range temporal dependencies between video snippets, and introduces a contrastive MIL learning that enforces large margins between the top- K normal and abnormal snippets.

detection is to identify the time window when an anomalous event happened – in the context of surveillance, examples of anomaly are bullying, shoplifting, violence, etc. It is challenging to collect and annotate large-scale data sets for anomaly detection given the rarity of anomaly events in surveillance videos. Therefore, most anomaly detection approaches rely on a training set containing exclusively videos of normal events to learn a distribution of normal activities, and during testing, these approaches classify frames that deviate from the learned distribution as anomaly [14, 15, 25, 27, 41, 42, 68]. Due to the lack of samples representing abnormal events, these approaches can fail to detect an anomalous event that has subtle differences compared with normal events [14] (e.g., shoplifting), leading to low anomaly detection accuracy. To alleviate this issue, recent studies explore a weakly-supervised setup using training samples with *video-level* label annotations of normal or abnormal [51, 59, 70]. This weakly-supervised setup targets a better anomaly classification accuracy at the expense of a relatively small human annotation effort.

Weakly supervised anomaly detection formulated as multiple instance learning (MIL) produces the current state-

of-the-art (SOTA) anomaly detection performance [51, 59, 66, 72]. Representing a video with a bag of video snippets, MIL-based methods aim to identify snippets where abnormal events occur. They assume that a normal video contains only normal snippets, while an anomalous video has one or more abnormal snippets, but we do not know where those snippets are. As shown in Fig. 1 (right), the current MIL-based methods aim to learn a larger anomaly score for the most abnormal snippet in the anomaly video than that in the normal video via a bag-wise ranking loss [51].

This formulation enables a good exploitation of the video-level labels. However, these methods have three major drawbacks. First, they rarely explore long and short-range temporal dependencies between snippets, even though abnormal events have shown to have strong temporal dependencies [25, 27, 59, 70]. Second, the number of abnormal video snippets varies significantly in different anomaly videos used for training, resulting in diverse amount of genuine anomaly supervisory information. However, current methods [51, 59, 70] tend to select only one snippet per video in their MIL learning. This restrictive snippet selection process often fails to get the genuine abnormal instances from the anomaly videos, and instead mistakenly selects a normal snippet from the anomaly video, introducing noise in the training process. By contrast, in videos that have many abnormal events, they fail to select all abnormal snippets. Third, guaranteeing a large margin between the representations of normal and anomalous instances is important, especially for discriminating hard examples (e.g., subtle anomalies) and for enabling better sample efficiency [13, 51]. However, current MIL methods [51, 59, 70] do not explicitly enforce this objective.

To address the three problems listed above, we propose a novel method, named Multi-scale Temporal Network trained with top- K Contrastive Multiple Instance Learning (MTN-KMIL). The top- K contrastive MIL is devised to enforce large margins between top-ranked K abnormal snippets in the positive bag (i.e., abnormal video) and that in the negative bag (i.e., normal video), as shown in Fig. 1 (right). The top- K instance selection results in substantially improved hit rate of abnormal snippets and thus better exploitation of the weak anomaly video labels. Further, MTN-KMIL defines ℓ_2 -norm of the feature representations of snippets as representation scores and optimises the representations by enforcing small ℓ_2 -norm for normal representations and large ℓ_2 -norm for abnormal representations. The anomaly scores of the snippets with top- K ℓ_2 -norms from respective normal and abnormal videos are then selected to be optimised by a binary cross entropy(BCE). By doing so, it unifies the optimisation of the representation learning and anomaly score learning, explicitly enforcing large margins between abnormal and normal snippets at the representation level and anomaly score level. To seamlessly incorporate long and short-range temporal dependen-

cies within each video, we introduce a Multi-scale Temporal Network (MTN) module that characterises multi-scale temporal dependencies with a pyramid of dilated convolutions (PDC) [64] over the time domain to explore multi-scale short-range temporal dependencies. PDC is used because of its strong capability in modelling spatial information [8]. Compared with the very recent graph convolutional network-based approaches [59, 70], our PDC-based method not only retains the positional distances between neighbouring snippets, but also preserves the sequential order with a multi-scale temporal receptive fields over consecutive snippets. Furthermore, MTN also contains a temporal self-attention module (TSA) to capture the long-range temporal dependency between video snippets. The PDC and TSA outputs are combined with the original video snippet features for final anomaly classification.

We validate our MTN-KMIL on three large-scale multi-scene anomaly detection benchmark data sets, namely ShanghaiTech [25], UCF-Crime [51], and XD-Violence [59]. We show that our method outperforms the current SOTA by 10.76% and 1.59% AUC on ShanghaiTech and UCF-Crime, respectively, and 2.4% AP on XD-Violence. We also show that our method achieves substantially better sample efficiency and subtle anomaly discriminability than popular MIL methods.

2. Related Work

Unsupervised Anomaly Detection. Traditional anomaly detection methods assume the availability of normal training data only and address the problem with one-class classification using handcrafted features [2, 29, 57, 67]. With the advent of deep learning, more recent approaches use the features from pre-trained deep neural networks [19, 36, 49, 69]. Others apply constraints on the latent space of normal manifold to learn compact normality representations [1, 3–5, 9, 11, 12, 28, 30, 37, 39, 44, 47, 56, 71]. Alternatively, some approaches depend on data reconstruction using generative models to learn the representations of normal samples by (adversarially) minimising the reconstruction error [6, 13, 18, 18, 25, 31, 32, 32, 33, 37, 43, 46, 47, 53, 60, 73]. These approaches assume that unseen anomalous videos/images often cannot be reconstructed well and consider samples of high reconstruction errors to be anomalies. However, due to the lack of prior knowledge of abnormality, these approaches can overfit the training data and fail to distinguish abnormal from normal events.

Weakly Supervised Anomaly Detection. Leveraging some labelled abnormal samples has shown substantially improved performance over the unsupervised approaches [24, 34, 35, 45, 51, 52, 59]. However, large-scale frame-level label annotation is too expensive to obtain. Hence, current SOTA video anomaly detection approaches rely on weakly supervised training that uses cheaper video-

level annotations. Sultani et al. [51] proposed the use of video-level labels and introduced the large-scale weakly-supervised video anomaly detection data set, UCF-Crime. Since then, weakly-supervised video anomaly detection has become a major research topic [54, 59, 66].

Weakly-supervised video anomaly detection methods are mainly based on the MIL framework [51]. However, most MIL-based methods [51, 66, 72] fail to leverage abnormal video labels as they can be affected by the label noise in the positive bag caused by a normal snippet mistakenly selected as the top abnormal event in an anomaly video. To deal with this problem, Zhong et al. [70] reformulated this problem as a binary classification under noisy label problem and used a graph convolution neural (GCN) network to clear the label noise. Although this paper shows more accurate results than [51], the training of GCN and MIL is computationally costly, and it can lead to unconstrained latent space (i.e., normal and abnormal features can lie at any place of the feature space) that can cause unstable performance. By contrast, our method has trivial computational overheads compared to the original MIL formulation. Moreover, our method unifies the representation learning and anomaly score learning by an ℓ_2 -norm-based contrastive learning, enabling better separation between normal and abnormal feature representations, improving the exploration of weak labels compared to previous MIL methods [51, 54, 59, 66, 70, 72].

Temporal Dependency has been explored in [22, 24, 25, 27, 59, 61, 70]. In anomaly detection, traditional methods [22, 61] convert consecutive frames into handcrafted motion trajectories to capture the local consistency between neighbouring frames. Diverse temporal dependency modelling methods have been used in deep anomaly detection approaches, such as stacked RNN [27], temporal consistency in future frame prediction [25], and convolution LSTM [24]. However, these methods capture short-range fixed-order temporal correlations only with single temporal scale, ignoring the long-range dependency from all possible temporal locations and the events with varying temporal length. GCN-based methods are explored in [59, 70] to capture the long-range dependency from snippets features, but they are inefficient and hard to train. By contrast, our MTN module can seamlessly and efficiently incorporate both the long and short-range temporal dependencies into our contrastive learning framework. Although MTN and self-attention networks have been studied for other tasks, such as image recognition [10, 16, 17, 55, 69], image captioning [62, 63] and video understanding [23, 58], this is the first work that synthesises MTN and self-attention networks to model the long and short-range temporal relations of video snippets for anomaly detection.

3. The Proposed Method: MTN-KMIL

Given a set of weakly-labelled training videos $\mathcal{D} = \{(\mathbf{V}_i, y_i)\}_{i=1}^{|\mathcal{D}|}$, where $\mathbf{V} \in \mathcal{V} \subset \mathbb{R}^{3 \times W \times H \times L}$ is a video containing L RGB frames of size $W \times H$ and is represented by a bag of T video snippets $\mathbf{V} = [\mathbf{S}_t]_{t=1}^T$, and $y \in \{0, 1\}$ denotes the video-level annotation ($y_i = 0$ if \mathbf{V}_i is a normal video and $y_i = 1$ otherwise), we aim to learn an anomaly detection function $f : \mathcal{V} \mapsto [0, 1]^T$ to classify each video snippet $\mathbf{S}_t \in \mathcal{S}$ into the abnormal or normal class. Following [51], we extract the features from \mathbf{V} for clips containing 16 frames. To guarantee that each video contains the same number of snippets, we divide the video into T snippets and compute the mean of all 16-frame clip level features within each snippet.

3.1. Architecture Overview

Our proposed MTN-KMIL method is depicted in Fig. 2, in which the multi-scale temporal network (MTN) module is designed to capture both long and short-range temporal relations between video snippets while the top- K contrastive MIL (KMIL) module is devised to make full use of the weak video labels to simultaneously and explicitly enforce class separability in both the feature representation and anomaly score levels. Particularly, the video features $\mathbf{X} \in \mathcal{X} \subset \mathbb{R}^{T \times D}$ (with T being the number of snippets, and D the number of feature dimensions) extracted from $[\mathbf{S}_t]_{t=1}^T$ are processed by MTN with a pyramid of dilated convolutions (PDC) using three dilation rates and with a temporal self-attention (TSA) component, with the output of TSA and each PDC dilation rate denoted by $\mathbf{X}^{(l)} \in \mathbb{R}^{T \times D/4}$, where $l \in \mathcal{L}$ and $\mathcal{L} = \{\text{PDC}_1, \text{PDC}_2, \text{PDC}_3, \text{TSA}\}$. Next, these features are concatenated to form $\tilde{\mathbf{X}} = [\mathbf{X}^{(l)}]_{l \in \mathcal{L}} \in \mathbb{R}^{T \times D}$ and fed into the KMIL module.

The KMIL module is a two-head network structure, with one head focusing on imposing large margins between the ℓ_2 -norm values of the normal and abnormal feature representations, while another head working on top- K MIL learning to guarantee the margin in the anomaly score level. Note that these two heads are optimised based on top- K snippets from respective abnormal and normal videos. The snippets from normal videos with the largest K anomaly scores represent hard negative examples, enabling better contrastive representation learning; meanwhile the use of top- K snippets from the anomalous videos increases the success rate of hitting genuine abnormal snippets, helping exploit the abnormal events of variable length better.

Our approach is an end-to-end framework represented by

$$\tilde{\mathbf{y}} = f_{\text{MTN-KMIL}}(\mathbf{X}; \theta_{\text{MTN-KMIL}}), \quad (1)$$

where $\tilde{\mathbf{y}} \in [0, 1]^T$ denotes the score for all video snippets (i.e., $\tilde{\mathbf{y}} = \{\tilde{y}_t\}_{t=1}^T$), and $f_{\text{MTN-KMIL}}(\cdot)$ represents the full neural network parameterised by $\theta_{\text{MTN-KMIL}}$.

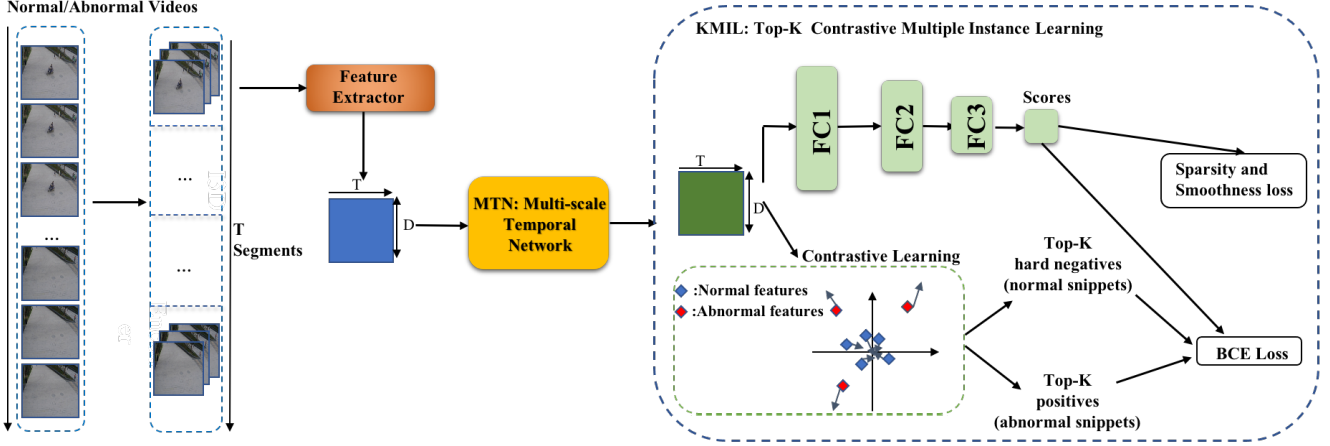


Figure 2. Our proposed MTN-KMIL divides each video into T segments (snippets) and extracts features with a pre-trained feature extractor. Then, we pass the T snippets features through the MTN module to capture the long and short-range temporal dependencies between snippets. The KMIL then selects the top- K hard negative normal and positive abnormal snippets based on features’ ℓ_2 -norm. The final top- K scores are trained with a BCE loss regularised by sparsity and smoothness constraints.

3.2. Feature Extraction

Following previous papers [51, 56, 59, 70], we use Inflated-3D (I3D) RGB [7] to extract the video features. Before extraction, we fix the frame rate as 24 fps and resize each frame to 240×360 . The I3D model is pre-trained on Kinetics [20] and we extract the feature from its ‘mix_5c’ layer. This feature extraction is performed as in $\mathbf{X} = f_{\text{I3D}}([\mathbf{S}_t]_{t=1}^T; \theta_{\text{I3D}})$, where $f_{\text{I3D}}(\cdot)$ denotes the I3D model, parameterised by θ_{I3D} , that receives all T video snippets $[\mathbf{S}_t]_{t=1}^T$, and \mathbf{X} represents the features extracted from the T video snippets, as defined above.

3.3. Multi-scale Temporal Network

Inspired by the attention techniques used in video understanding [23, 58], our proposed MTN captures the multi-scale temporal dependencies of video snippets and the global temporal dependencies between video snippets, as displayed in Fig. 3. More specifically, MTN uses a pyramid of dilated convolutions over the time domain to learn multi-scale representations for video snippets. Dilated convolution is usually applied in the spatial domain with the goal of expanding the the receptive field without losing resolution [64]. For video anomaly detection, it is important to capture the multi-scale temporal dependencies of neighbouring video snippets, so we propose the use of dilated convolution over the temporal dimension. Given the snippet feature $\mathbf{X}_d \in \mathbb{R}^T$, the 1-D dilated convolution operation with kernel $\mathbf{W}_{k,d}^{(l)} \in \mathbb{R}^W$ with $k \in \{1, \dots, D/4\}$, $d \in \{1, \dots, D\}$, $l \in \{\text{PDC}_1, \text{PDC}_2, \text{PDC}_3\}$, and W denoting the filter size, is defined by

$$\mathbf{X}_k^{(l)} = \sum_{d=1}^D \mathbf{W}_{k,d}^{(l)} *^{(l)} \mathbf{X}_d, \quad (2)$$

where $*^{(l)}$ represents the dilated convolution operator indexed by l , $\mathbf{X}_k^{(l)} \in \mathbb{R}^T$ represents the output features after applying the dilated convolution over the temporal dimension. The dilation factors for $\{\text{PDC}_1, \text{PDC}_2, \text{PDC}_3\}$ are $\{1, 2, 4\}$, respectively, as depicted in Fig. 3.

The global temporal dependencies between video snippets is achieved with a self-attention module, which has shown promising performance on capturing the long-range spatial dependency on video understanding [58], image classification [69] and object detection [40]. Motivated by the previous works using GCN to model global temporal information [59, 70], we re-formulate spatial self-attention technique to work on the time dimension and capture global temporal context modelling. In detail, we aim to produce an attention map $\mathbf{M} \in \mathbb{R}^{T \times T}$ that estimates the pairwise correlation between snippets. Our TSA module first uses a 1×1 convolution to reduce the spatial dimension from $\mathbf{X} \in \mathbb{R}^{T \times D}$ to $\mathbf{X}^{(c)} \in \mathbb{R}^{T \times D/4}$ with $\mathbf{X}^{(c)} = \text{Conv}_{1 \times 1}(\mathbf{X})$. We then apply three separate 1×1 convolution layers to $\mathbf{X}^{(c)}$ to produce $\mathbf{X}^{(c1)}, \mathbf{X}^{(c2)}, \mathbf{X}^{(c3)} \in \mathbb{R}^{T \times D/4}$, as in $\mathbf{X}^{(ci)} = \text{Conv}_{1 \times 1}(\mathbf{X}^{(c)})$ for $i \in \{1, 2, 3\}$. The attention map is then built with $\mathbf{M} = (\mathbf{X}^{(c1)} (\mathbf{X}^{(c2)})^\top)$, which produces $\mathbf{X}^{(c4)} = \text{Conv}_{1 \times 1}(\mathbf{M} \mathbf{X}^{(c3)})$. A skip connection is added after this final 1×1 convolutional layer, as in

$$\mathbf{X}^{(\text{TSA})} = \mathbf{X}^{(c4)} + \mathbf{X}^{(c)}. \quad (3)$$

The output from the MTN is formed with a concatenation of the outputs from the PDC and MTN modules $\bar{\mathbf{X}} = [\mathbf{X}^{(l)}]_{l \in \mathcal{L}} \in \mathbb{R}^{T \times D}$, with $\mathcal{L} = \{\text{PDC}_1, \text{PDC}_2, \text{PDC}_3, \text{TSA}\}$. A skip connection using the original features \mathbf{X} produces the final output

$$\mathbf{X}^{(\text{MTN})} = \bar{\mathbf{X}} + \mathbf{X}. \quad (4)$$

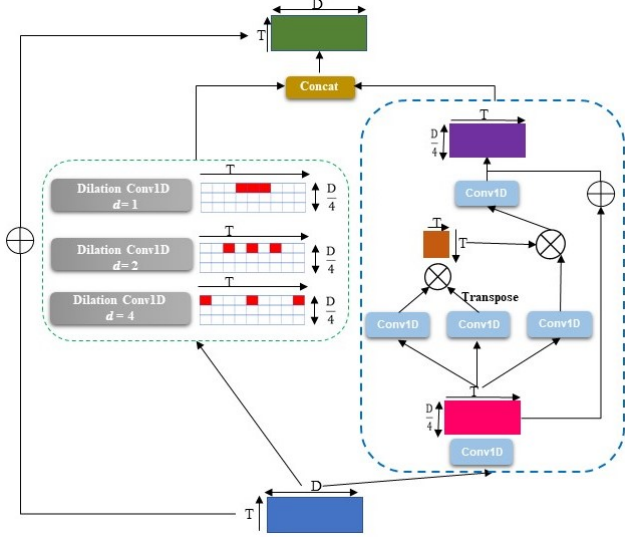


Figure 3. Our proposed MTN, consisting of two modules. The module on the left uses the pyramid dilated convolutions to capture the local consecutive snippets dependency over different temporal scales. The module on the right relies on a self-attention network to compute the global temporal correlations. The features from the two modules are concatenated to produce the MTN output.

3.4. Top- K Contrastive Multiple Instance Learning

Anomalous events are usually hard to capture and to define due to their unpredictability in terms of environment, appearance and dynamics [51]. Hence, one the major challenges of weakly supervised anomaly detection is how to detect anomalous snippets from a whole video labelled as abnormal given that the majority of snippets from an abnormal video consist of normal events. Furthermore, the training process for a weakly supervised anomaly detector is extremely imbalanced given that all snippets from normal videos and the majority of snippets from abnormal videos are normal. On top of that, even though the majority of normal videos are easy to fit, they can overwhelm the training process and challenge the fitting of the few abnormal snippets. In other words, even if abnormal events can have individual high losses, their sum is too small compared with the sum of the losses from normal events that have already been fit by the model.

We propose a solution for the issues mentioned above using the top- K normal and abnormal snippets with the highest ℓ_2 -norm of $\mathbf{X}^{(\text{MTN})}$ from (4) at each training iteration. This solution implies that the training set will be naturally balanced with the same number of samples for the normal and abnormal classes, solving the imbalanced training problem. The K normal video snippets with highest ℓ_2 -norm represent the most challenging normal samples to be fit by the model, so this means that the training process will not stagnate with easy-to-fit normal snippets. The top- K ab-

normal video snippets can solve two issues: 1) selecting K snippets almost guarantees that an abnormal snippet will be included in the training set of abnormal events (e.g., say the probability of an abnormal event is p in a video, then the probability of including it in the top- K set is $1 - (1 - p)^K$); and 2) if the abnormal event lasts for more than one snippet, our top- K abnormal video snippets set can include more samples for training. A potential issue with our approach is that normal events can be included in the top- K abnormal snippets and bias the training process. This issue is mitigated by the training of the K most challenging normal events, and in practice, we observed that the process is robust to these eventual normal snippets in the abnormal set.

We propose a contrastive loss to pull the snippets representations with K largest ℓ_2 -norm values from normal bags close to zero, and push the representations with K largest ℓ_2 -norm values from abnormal bags farther than a margin away from zero. More specifically, we propose the following loss:

$$\mathcal{L}_c = \max\left(0, m - \frac{1}{K} \sum_{j=1}^K K_{\max}(\mathcal{B}^{(a)}) + \frac{1}{K} \sum_{j=1}^K K_{\max}(\mathcal{B}^{(n)})\right), \quad (5)$$

where $\mathcal{B}^{(a)} = \{\|\mathbf{X}_t^{\text{MTN}}\|_2\}_{t=1}^T$ denotes the set of ℓ_2 norms of MTN features for the T video snippets annotated as abnormal (a) (similarly for the normal set $\mathcal{B}^{(n)}$), $K_{\max}(\mathcal{B})$ returns a set containing the largest K elements within the set \mathcal{B} , and m is the pre-defined margin.

3.5. Classification Loss Function

For the optimisation of the anomaly scores, the classification loss function comprises three different functions, defined below.

Binary Cross Entropy: We use the binary cross entropy (BCE) loss to train the top- K anomaly scores selected from normal and abnormal sets $\mathcal{B}^{(n)}$, $\mathcal{B}^{(a)}$ defined in (5), as follows:

$$\mathcal{L}_b = -(y \log(\tilde{y}_t) + (1 - y) \log(1 - \tilde{y}_t)), \quad (6)$$

where \tilde{y}_t is the output of the snippet $t \in \{1, \dots, T\}$ from MTN-KMIL defined in (1), and $y \in \{0, 1\}$ is the video-level annotation.

Smoothness and Sparsity Loss: Inspired by [51], we apply the temporal smoothness and sparsity losses for the snippets from abnormal videos, given that anomalous and normal events tend to be temporally consistent. The smoothness loss is defined as:

$$\mathcal{L}_{sm} = \frac{1}{T} \sum_{t=2}^T (\tilde{y}_t - \tilde{y}_{t-1})^2, \quad (7)$$

for the videos labelled with $y = 1$ (i.e., this loss is applied only to abnormal videos). The sparsity loss is based on the

assumption that anomalous snippets are rare events in abnormal videos. Hence, this loss enforces that only a small number of contiguous snippets are classified as abnormal. The sparsity loss is defined as:

$$\mathcal{L}_{sp} = \frac{1}{T} \sum_{t=1}^T |\tilde{y}_t|. \quad (8)$$

The overall loss is defined as follows:

$$\mathcal{L}_{overall} = \mathcal{L}_b + \mathcal{L}_c + \alpha \mathcal{L}_{sm} + \beta \mathcal{L}_{sp}, \quad (9)$$

where α and β weights the sparsity and smoothness terms.

4. Experiments

4.1. Data Sets and Evaluation Metric

ShanghaiTech is a medium-scale data set from fixed-angle street video surveillance. It has 13 different background scenes and 437 videos, including 307 normal videos and 130 anomaly videos. The original data set [25] is a popular benchmark for the anomaly detection task that assumes the availability of normal training data. Zhong et al. [70] reorganised the data set by selecting a subset of anomalous testing videos into training data to build a weakly supervised training set, so that both training and testing sets cover all 13 background scenes. Our experiments are performed on this weakly supervised ShanghaiTech data set as in [54, 66, 70].

UCF-Crime is a large-scale anomaly detection data set [51]. It contains 1900 untrimmed videos with a total duration of 128 hours from real-world street and indoor surveillance cameras. Unlike the static backgrounds in ShanghaiTech, UCF-Crime consists of complicated and diverse backgrounds. Both training and testing sets contain the same number of normal and abnormal videos. The data set covers 13 classes of anomalies in 1,610 training videos with video-level labels and 290 test videos with frame-level labels.

XD-Violence is a recently proposed large-scale multi-scene anomaly detection data set, collected from real life movies, online videos, sport streaming, surveillance cameras and CCTVs [59]. The total duration of this data set is over 217 hours, containing 4754 untrimmed videos with video-level labels in the training set and frame-level labels in the testing set. It is currently the largest publicly available video anomaly detection data set.

Evaluation Metric. Similarly to previous papers [13, 25, 51, 54, 66], we use the frame-level area under the ROC curve (AUC) as the evaluation metric for all data sets. Moreover, following [59], we also use average precision (AP) as the evaluation metric for the XD-Violence data set. Larger AUC and AP values indicate better performance.

4.2. Implementation Details

Following [51], each video is divided into 32 video snippets, i.e., $T = 32$. For all experiments, we set the contrastive learning margin $m = 100$, $K = 3$ in (5), and the weights for the sparsity and smoothness terms in (9) are set as $\alpha = 8 \times 10^{-4}$ and $\beta = 8 \times 10^{-3}$. The three FC layers described in the model (Sec. 3.1) have 512, 128 and 1 nodes, where each of those FC layers is followed by a ReLU activation function and a dropout function with a dropout rate of 0.7. The 2048D features are extracted from the 'mix_5c' layer of the pre-trained I3D network. In MTN, we set the pyramid dilate rate as 1, 2 and 4, and we use the 3×1 Conv1D for each dilated convolution branch. For the self-attention block, we use a 1×1 Conv1D.

Our model MTN-KMIL is trained in an end-to-end manner using the Adam optimiser [21] with a weight decay of 0.0005 and a batch size of 64 for 50 epochs. The learning rate is set to 0.001 for ShanghaiTech and UCF-Crime, and 0.0001 for XD-Violence. Each mini-batch consists of samples from 32 randomly selected normal and abnormal videos. The method is implemented using PyTorch [38].

4.3. Results on ShanghaiTech

The frame-level AUC result on ShanghaiTech is shown in Tab. 1. Our method MTN-KMIL achieves superior performance when compared with previous SOTA unsupervised learning methods [14, 25, 27, 37, 65] and weakly-supervised approaches [54, 66, 70]. With I3D features, our model obtains the best AUC result on this data set: 96.14%. This outperforms [66] by around 14% when using the same I3D-RGB features; it outperforms [54] by at least 4.9% using I3D-RGB, I3D-Flow, or both features. Moreover, we retrain the DeepMIL method in [51] using the same I3D features. The result shows that our approach is better by a large 10.81% gap. Our method shows better AUC results than the GCN-based weakly-supervised method in [70] by a 11.7% margin, which indicates that our MTN is more effective at capturing temporal dependencies than GCN.

Supervision	Method	Feature	AUC(%)
Unsupervised	Conv-AE [14]	-	60.85
	Stacked-RNN [27]	-	68.0
	Frame-Pred [25]	-	73.4
	Mem-AE [13]	-	71.2
	MNAD [37]	-	70.5
	VEC [65]	-	74.8
Weakly Supervised	GCN-Anomaly [70]	C3D-RGB	76.44
	GCN-Anomaly [70]	TSN-Flow	84.13
	GCN-Anomaly [70]	TSN-RGB	84.44
	Zhang et al. [66]	I3D-RGB	82.50
	Sultani et al.* [51]	I3D RGB	85.33
	AR-Net [54]	I3D Flow	82.32
	AR-Net [54]	I3D-RGB	85.38
	AR-Net [54]	I3D-RGB & I3D Flow	91.24
	Ours	I3D-RGB	96.14

Table 1. Comparison of frame-level AUC performance with other SOTA un/weakly-supervised methods on ShanghaiTech. * indicates we retrain the method in [51] using I3D features.

4.4. Results on UCF-Crime

The AUC results on UCF-Crime are shown in Tab. 2. Our method substantially outperforms all previous unsupervised learning approaches [14,27,50,56]. Particularly, using the same I3D-RGB features, we surpass the current SOTA BODS and GODS [56] by at least 13%. Remarkably, compared to the weakly-supervised MIL-based methods by Sultani et al. [51], Zhang et al. [66], Zhu et al. [72] and Wu et al. [59], our method outperforms them by 8.62%, 5.37%, 5.03% and 1.59%, respectively. Zhong et al. [70] use a computationally costly alternating training scheme to achieve an AUC of 82.12%, while our method utilises an efficient end-to-end training scheme and outperforms Zhong et al. [70] by 1.91%.

Supervision	Method	Feature	AUC (%)
Unsupervised	SVM Baseline	-	50.00
	Conv-AE [14]	-	50.60
	Sohrab et al. [50]	-	58.50
	Lu et al. [26]	C3D RGB	65.51
	BODS [56]	I3D RGB	68.26
	GODS [56]	I3D RGB	70.46
Weakly Supervised	Sultani et al. [51]	C3D RGB	75.41
	Sultani et al.* [51]	I3D RGB	77.92
	Zhang et al. [66]	C3D RGB	78.66
	Motion-Aware [72]	PWC Flow	79.00
	GCN-Anomaly [70]	C3D RGB	81.08
	GCN-Anomaly [70]	TSN Flow	78.08
	GCN-Anomaly [70]	TSN RGB	82.12
	Wu et al. [59]	I3D RGB	82.44
	Ours	I3D RGB	84.03

Table 2. Frame-level AUC performance on UCF-Crime. * indicates we retrain the method in [51] using I3D features.

4.5. Results on XD-Violence

XD-Violence is a recently released data set, on which few results have been reported, as displayed in Tab. 3. Our approach surpasses all unsupervised learning approaches by a minimum of 27.03% in AP. Comparing with SOTA weakly-supervised methods [51, 59], our method is 2.4% and 2.13% better than Wu et al. [59] and Sultani et al. [51], using the same I3D features.

Supervision	Method	Feature	AP(%)
Unsupervised	SVM baseline	-	50.78
	OCSVM [48]	-	27.25
	Hasan et al. [14]	-	30.77
Weakly Supervised	Sultani et al. [51]	C3D RGB	73.20
	Sultani et al.* [51]	I3D RGB	75.68
	Wu et al. [59]	I3D RGB	75.41
	Ours	I3D RGB	77.81

Table 3. Comparison of frame-level AUC performance with other SOTA un/weakly-supervised methods on XD-Violence. * indicates we retrain the method in [51] using I3D features.

4.6. Sample Efficiency Analysis

We further investigate the sample efficiency of our method by looking into its performance w.r.t. the number of abnormal videos used in the training. The experiment is conducted on ShanghaiTech. We reduce the number of abnormal training videos from the original 63 videos down to 25 videos, with the normal training videos and test data fixed. The MIL method in [51] is used as a baseline. For the sake of fair comparison, the same I3D features are used in both methods. The AUC results are shown in Fig. 5. As expected, the performance of both our method and Sultani et al. [51] decreases with decreasing number of abnormal training videos. The decreasing rates of our model are relatively smaller than Sultani et al. [51], indicating the robustness of our MTN-KMIL. Remarkably, our method using only 25 abnormal training videos outperforms [51] using all 63 abnormal videos by about 4%, i.e., although our method uses 60% less labelled abnormal training videos, it can still substantially outperform Sultani et al. [51].

4.7. Subtle Anomaly Discriminability

We also examine the capability of our method in discriminating subtle abnormal events from normal activities. UCF-Crime contains multiple such anomaly classes. Thus, we perform the experiment on UCF-Crime by looking into the AUC performance on each individual anomaly class. The models are trained on the full training data and we use [51] as baseline. The results are shown in Fig. 6. Our model shows remarkable performance on human-centric abnormal events, even when the abnormality is very subtle. Particularly, our method outperforms Sultani et al. [51] in 8 human-centric anomaly classes (i.e., arson, assault, burglary, robbery, shooting, shoplifting, stealing, vandalism), significantly lifting the AUC performance by 10% to 15% in subtle anomaly classes such as burglary, shoplifting, vandalism. For the arrest, fighting, road accidents and explosion classes, our method shows competitive performance to [51]. Our model is less effective in the abuse class because this class contains overwhelming human-centric abuse events in the training data but its testing videos contain animal abuse events only.

4.8. Ablation Studies

We perform the ablation study on ShanghaiTech, as shown in Tab. 4. The baseline model replaces PDC and TSA with a 1×1 convolutional layer and is trained with the original MIL approach as in [51]. The resulting model achieves only 85.96% AUC on ShanghaiTech (a result similar to the one in [51]). By adding PDC or TSA, the AUC performance is boosted to 89.21% and 91.73%, respectively. When both PDC and TSA are added, the AUC result increases to 92.32%. This indicates that PDC and TSA contributes to the overall performance, and they also complement each other in capturing both long and short-range

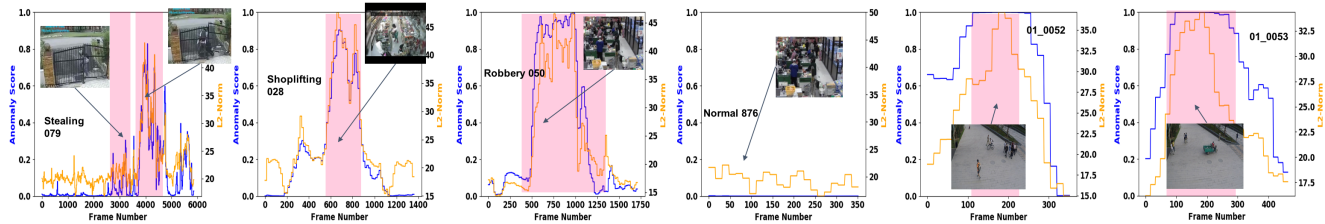


Figure 4. Anomaly scores and ℓ_2 -norm values of our method on UCF-Crime (*stealing079,shoplifting028,robbery050 normal876*), and ShanghaiTech (*01_0052, 01_0053*) test videos. Pink areas indicate the manually labelled abnormal events.

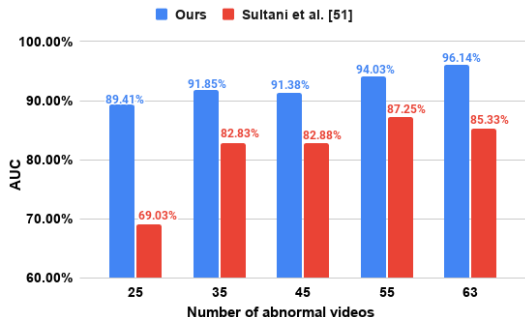


Figure 5. AUC w.r.t. the number of abnormal training videos.

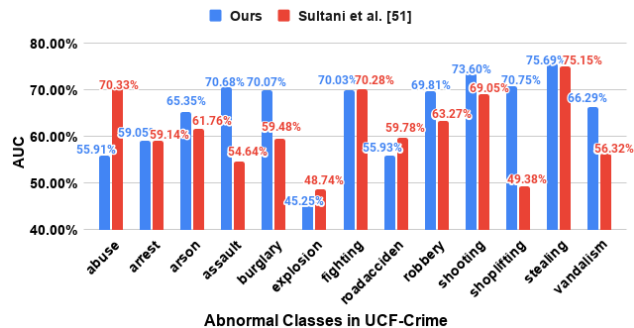


Figure 6. AUC results w.r.t. individual classes on UCF-Crime.

temporal relations. When adding only the KMIL module to the baseline, the AUC substantially increases by over 7%, indicating that our top- K contrastive MIL considerably improves over the original MIL method as it enables better exploitation of the labelled abnormal video data. Additionally, combining either PDC or TSA with KMIL helps further improve the performance. Then, the full model MTN-KMIL can achieve the best performance of 96.14%.

4.9. Qualitative Analysis

In Fig. 4, we show the anomaly scores produced by our model for diverse test videos from UCF-Crime and ShanghaiTech. Three anomalous videos and one normal video from UCF-Crime are used (*stealing079, shoplifting028, robbery050* and *normal876*). As illustrated by the

Baseline	PDC	TSA	KMIL	AUC (%) - Shanghai
✓				85.96
✓	✓			89.21
✓		✓		91.73
✓	✓	✓		92.32
✓			✓	92.99
✓		✓	✓	94.63
✓	✓		✓	93.91
✓	✓	✓	✓	96.14

Table 4. Ablation studies of our method on ShanghaiTech.

ℓ_2 -norm value curve (i.e., orange curves), our top- K MIL module can effectively produce a small ℓ_2 -norm for normal snippets and a large ℓ_2 -norm for abnormal snippets. Furthermore, our model can successfully ensure large margins between the anomaly scores of the normal and abnormal snippets (i.e., blank and pink shadowed areas, respectively). Our model is also able to detect multiple anomalous events in one video (e.g., *stealing079*), which makes the problem more difficult. Also, for the anomalous events *stealing* and *shoplifting*, the abnormality is subtle and barely seen through the videos, but our model can still detect it. Moreover, we also show the anomaly scores and feature ℓ_2 -norms produced by our model for *01_0052* and *01_0053* from ShanghaiTech (last two figures in Fig. 4). Our model can effectively output high anomaly scores for anomalous events of vehicle entering.

5. Conclusion

To conclude, we present a new video anomaly detection model under weak supervision, named as MTN-KMIL. Two key insights we found empirically are as follows: 1) simultaneously learning the complementary long and short-range temporal relations through the end-to-end training framework is crucial for video anomaly detection, e.g., resulting in over 6% AUC improvement as in Tab. 4, and 2) explicitly enforcing large margins between abnormal and normal instances in both the representation and anomaly score levels enables substantially better exploitation of the weak annotations (e.g., MTN-KMIL uses 60% less labelled abnormal data yet achieves better performance than its contender) and discriminability in identifying diverse types of subtle anomalies. These two key aspects are achieved in the MTN

and KMIL modules in our method, respectively.

References

- [1] Davide Abati, Angelo Porrello, Simone Calderara, and Rita Cucchiara. Latent space autoregression for novelty detection. In *Proceedings of the IEEE/CVF Conference on Computer Vision and Pattern Recognition (CVPR)*, June 2019. [2](#)
- [2] Arslan Basharat, Alexei Gritai, and Mubarak Shah. Learning object motion patterns for anomaly detection and improved object detection. In *2008 IEEE Conference on Computer Vision and Pattern Recognition*, pages 1–8. IEEE, 2008. [2](#)
- [3] Liron Bergman and Yedid Hoshen. Classification-based anomaly detection for general data. *arXiv preprint arXiv:2005.02359*, 2020. [2](#)
- [4] Paul Bergmann, Michael Fauser, David Sattlegger, and Carsten Steger. Mvtec ad – a comprehensive real-world dataset for unsupervised anomaly detection. In *Proceedings of the IEEE/CVF Conference on Computer Vision and Pattern Recognition (CVPR)*, June 2019. [2](#)
- [5] Paul Bergmann, Michael Fauser, David Sattlegger, and Carsten Steger. Uninformed students: Student-teacher anomaly detection with discriminative latent embeddings. In *IEEE/CVF Conference on Computer Vision and Pattern Recognition (CVPR)*, June 2020. [2](#)
- [6] Philippe Burlina, Neil Joshi, and I-Jeng Wang. Where’s wally now? deep generative and discriminative embeddings for novelty detection. In *Proceedings of the IEEE/CVF Conference on Computer Vision and Pattern Recognition (CVPR)*, June 2019. [2](#)
- [7] Joao Carreira and Andrew Zisserman. Quo vadis, action recognition? a new model and the kinetics dataset. In *proceedings of the IEEE Conference on Computer Vision and Pattern Recognition*, pages 6299–6308, 2017. [4](#)
- [8] Liang-Chieh Chen, George Papandreou, Iasonas Kokkinos, Kevin Murphy, and Alan L Yuille. Deeplab: Semantic image segmentation with deep convolutional nets, atrous convolution, and fully connected crfs. *IEEE transactions on pattern analysis and machine intelligence*, 40(4):834–848, 2017. [2](#)
- [9] Kai-Wen Cheng, Yie-Tarng Chen, and Wen-Hsien Fang. Video anomaly detection and localization using hierarchical feature representation and gaussian process regression. In *Proceedings of the IEEE Conference on Computer Vision and Pattern Recognition (CVPR)*, June 2015. [2](#)
- [10] Jifeng Dai, Haozhi Qi, Yuwen Xiong, Yi Li, Guodong Zhang, Han Hu, and Yichen Wei. Deformable convolutional networks. In *Proceedings of the IEEE international conference on computer vision*, pages 764–773, 2017. [3](#)
- [11] Allison Del Giorno, J Andrew Bagnell, and Martial Hebert. A discriminative framework for anomaly detection in large videos. In *European Conference on Computer Vision*, pages 334–349. Springer, 2016. [2](#)
- [12] Izhak Golan and Ran El-Yaniv. Deep anomaly detection using geometric transformations. In *Advances in Neural Information Processing Systems*, pages 9758–9769, 2018. [2](#)
- [13] Dong Gong, Lingqiao Liu, Vuong Le, Budhaditya Saha, Moussa Reda Mansour, Svetha Venkatesh, and Anton van den Hengel. Memorizing normality to detect anomaly: Memory-augmented deep autoencoder for unsupervised anomaly detection. In *Proceedings of the IEEE International Conference on Computer Vision*, pages 1705–1714, 2019. [2](#), [6](#)
- [14] Mahmudul Hasan, Jonghyun Choi, Jan Neumann, Amit K Roy-Chowdhury, and Larry S Davis. Learning temporal regularity in video sequences. In *Proceedings of the IEEE conference on computer vision and pattern recognition*, pages 733–742, 2016. [1](#), [6](#), [7](#)
- [15] Ryota Hinami, Tao Mei, and Shin’ichi Satoh. Joint detection and recounting of abnormal events by learning deep generic knowledge. In *Proceedings of the IEEE International Conference on Computer Vision*, pages 3619–3627, 2017. [1](#)
- [16] Jie Hu, Li Shen, Samuel Albanie, Gang Sun, and Andrea Vedaldi. Gather-excite: Exploiting feature context in convolutional neural networks. In *Advances in neural information processing systems*, pages 9401–9411, 2018. [3](#)
- [17] Jie Hu, Li Shen, and Gang Sun. Squeeze-and-excitation networks. In *Proceedings of the IEEE conference on computer vision and pattern recognition*, pages 7132–7141, 2018. [3](#)
- [18] Radu Tudor Ionescu, Fahad Shahbaz Khan, Mariana-Juliana Georgescu, and Ling Shao. Object-centric auto-encoders and dummy anomalies for abnormal event detection in video. In *Proceedings of the IEEE Conference on Computer Vision and Pattern Recognition*, pages 7842–7851, 2019. [2](#)
- [19] Radu Tudor Ionescu, Sorina Smeureanu, Bogdan Alexe, and Marius Popescu. Unmasking the abnormal events in video. In *Proceedings of the IEEE International Conference on Computer Vision*, pages 2895–2903, 2017. [2](#)
- [20] Will Kay, Joao Carreira, Karen Simonyan, Brian Zhang, Chloe Hillier, Sudheendra Vijayanarasimhan, Fabio Viola, Tim Green, Trevor Back, Paul Natsev, et al. The kinetics human action video dataset. *arXiv preprint arXiv:1705.06950*, 2017. [4](#)
- [21] Diederik P Kingma and Jimmy Ba. Adam: A method for stochastic optimization. *arXiv preprint arXiv:1412.6980*, 2014. [6](#)
- [22] Louis Kratz and Ko Nishino. Anomaly detection in extremely crowded scenes using spatio-temporal motion pattern models. In *2009 IEEE Conference on Computer Vision and Pattern Recognition*, pages 1446–1453. IEEE, 2009. [3](#)
- [23] C. Liu, X. Xu, and Y. Zhang. Temporal attention network for action proposal. In *2018 25th IEEE International Conference on Image Processing (ICIP)*, pages 2281–2285, 2018. [3](#), [4](#)
- [24] Wen Liu, Weixin Luo, Zhengxin Li, Peilin Zhao, Shenghua Gao, et al. Margin learning embedded prediction for video anomaly detection with a few anomalies. [2](#), [3](#)
- [25] Wen Liu, Weixin Luo, Dongze Lian, and Shenghua Gao. Future frame prediction for anomaly detection—a new baseline. In *Proceedings of the IEEE Conference on Computer Vision and Pattern Recognition*, pages 6536–6545, 2018. [1](#), [2](#), [3](#), [6](#)
- [26] Cewu Lu, Jianping Shi, and Jiaya Jia. Abnormal event detection at 150 fps in matlab. In *Proceedings of the IEEE international conference on computer vision*, pages 2720–2727, 2013. [7](#)
- [27] Weixin Luo, Wen Liu, and Shenghua Gao. A revisit of sparse coding based anomaly detection in stacked rnn framework. In *Proceedings of the IEEE International Conference on Computer Vision*, pages 341–349, 2017. [1](#), [2](#), [3](#), [6](#), [7](#)

- [28] Amir Markovitz, Gilad Sharir, Itamar Friedman, Lih Zelnik-Manor, and Shai Avidan. Graph embedded pose clustering for anomaly detection. In *IEEE/CVF Conference on Computer Vision and Pattern Recognition (CVPR)*, June 2020. 2
- [29] Gérard Medioni, Isaac Cohen, François Brémont, Somboon Hongeng, and Ramakant Nevatia. Event detection and analysis from video streams. *IEEE Transactions on pattern analysis and machine intelligence*, 23(8):873–889, 2001. 2
- [30] Romero Morais, Vuong Le, Truyen Tran, Budhaditya Saha, Moussa Mansour, and Svetha Venkatesh. Learning regularity in skeleton trajectories for anomaly detection in videos. In *Proceedings of the IEEE/CVF Conference on Computer Vision and Pattern Recognition (CVPR)*, June 2019. 2
- [31] Romero Morais, Vuong Le, Truyen Tran, Budhaditya Saha, Moussa Mansour, and Svetha Venkatesh. Learning regularity in skeleton trajectories for anomaly detection in videos. In *Proceedings of the IEEE Conference on Computer Vision and Pattern Recognition*, pages 11996–12004, 2019. 2
- [32] Duc Tam Nguyen, Zhongyu Lou, Michael Klar, and Thomas Brox. Anomaly detection with multiple-hypotheses predictions. In *International Conference on Machine Learning*, pages 4800–4809. PMLR, 2019. 2
- [33] Trong-Nguyen Nguyen and Jean Meunier. Anomaly detection in video sequence with appearance-motion correspondence. In *Proceedings of the IEEE/CVF International Conference on Computer Vision (ICCV)*, October 2019. 2
- [34] Guansong Pang, Longbing Cao, Ling Chen, and Huan Liu. Learning representations of ultrahigh-dimensional data for random distance-based outlier detection. In *Proceedings of the 24th ACM SIGKDD International Conference on Knowledge Discovery & Data Mining*, pages 2041–2050, 2018. 2
- [35] Guansong Pang, Chunhua Shen, and Anton van den Hengel. Deep anomaly detection with deviation networks. In *Proceedings of the 25th ACM SIGKDD International Conference on Knowledge Discovery & Data Mining*, pages 353–362, 2019. 2
- [36] Guansong Pang, Cheng Yan, Chunhua Shen, Anton van den Hengel, and Xiao Bai. Self-trained deep ordinal regression for end-to-end video anomaly detection. In *Proceedings of the IEEE/CVF Conference on Computer Vision and Pattern Recognition*, pages 12173–12182, 2020. 2
- [37] Hyunjong Park, Jongyoun Noh, and Bumsu Ham. Learning memory-guided normality for anomaly detection. In *IEEE/CVF Conference on Computer Vision and Pattern Recognition (CVPR)*, June 2020. 2, 6
- [38] Adam Paszke, Sam Gross, Francisco Massa, Adam Lerer, James Bradbury, Gregory Chanan, Trevor Killeen, Zeming Lin, Natalia Gimelshein, Luca Antiga, Alban Desmaison, Andreas Kopf, Edward Yang, Zachary DeVito, Martin Raison, Alykhan Tejani, Sasank Chilamkurthy, Benoit Steiner, Lu Fang, Junjie Bai, and Soumith Chintala. Pytorch: An imperative style, high-performance deep learning library. In H. Wallach, H. Larochelle, A. Beygelzimer, F. d Alché-Buc, E. Fox, and R. Garnett, editors, *Advances in Neural Information Processing Systems 32*, pages 8024–8035. Curran Associates, Inc., 2019. 6
- [39] Pramuditha Perera, Ramesh Nallapati, and Bing Xiang. Ocgan: One-class novelty detection using gans with constrained latent representations. In *Proceedings of the IEEE/CVF Conference on Computer Vision and Pattern Recognition (CVPR)*, June 2019. 2
- [40] Hughes Perreault, Guillaume-Alexandre Bilodeau, Nicolas Saunier, and Maguelonne Héritier. Spotnet: Self-attention multi-task network for object detection. In *2020 17th Conference on Computer and Robot Vision (CRV)*, pages 230–237. IEEE, 2020. 4
- [41] Mahdyar Ravanbakhsh, Moin Nabi, Hossein Mousavi, Enver Sangineto, and Nicu Sebe. Plug-and-play cnn for crowd motion analysis: An application in abnormal event detection. In *2018 IEEE Winter Conference on Applications of Computer Vision (WACV)*, pages 1689–1698. IEEE, 2018. 1
- [42] Mahdyar Ravanbakhsh, Moin Nabi, Enver Sangineto, Lucio Marcenaro, Carlo Regazzoni, and Nicu Sebe. Abnormal event detection in videos using generative adversarial nets. In *2017 IEEE International Conference on Image Processing (ICIP)*, pages 1577–1581. IEEE, 2017. 1
- [43] Huamin Ren, Weifeng Liu, Søren Ingvor Olsen, Sergio Escalera, and Thomas B Moeslund. Unsupervised behavior-specific dictionary learning for abnormal event detection. In *BMVC*, pages 28–1, 2015. 2
- [44] Lukas Ruff, Robert Vandermeulen, Nico Goernitz, Lucas Deecke, Shoaib Ahmed Siddiqui, Alexander Binder, Emmanuel Müller, and Marius Kloft. Deep one-class classification. In *International conference on machine learning*, pages 4393–4402, 2018. 2
- [45] Lukas Ruff, Robert A Vandermeulen, Nico Görnitz, Alexander Binder, Emmanuel Müller, Klaus-Robert Müller, and Marius Kloft. Deep semi-supervised anomaly detection. *arXiv preprint arXiv:1906.02694*, 2019. 2
- [46] Mohammad Sabokrou, Mohsen Fayyaz, Mahmood Fathy, and Reinhard Klette. Deep-cascade: Cascading 3d deep neural networks for fast anomaly detection and localization in crowded scenes. *IEEE Transactions on Image Processing*, 26(4):1992–2004, 2017. 2
- [47] Mohammad Sabokrou, Mohammad Khalooei, Mahmood Fathy, and Ehsan Adeli. Adversarially learned one-class classifier for novelty detection. In *Proceedings of the IEEE Conference on Computer Vision and Pattern Recognition (CVPR)*, June 2018. 2
- [48] Bernhard Schölkopf, Robert C Williamson, Alex J Smola, John Shawe-Taylor, and John C Platt. Support vector method for novelty detection. In *Advances in neural information processing systems*, pages 582–588, 2000. 7
- [49] Sorina Smeureanu, Radu Tudor Ionescu, Marius Popescu, and Bogdan Alexe. Deep appearance features for abnormal behavior detection in video. In *International Conference on Image Analysis and Processing*, pages 779–789. Springer, 2017. 2
- [50] Fahad Sohrab, Jenni Raitoharju, Moncef Gabbouj, and Alexandros Iosifidis. Subspace support vector data description. In *2018 24th International Conference on Pattern Recognition (ICPR)*, pages 722–727. IEEE, 2018. 7
- [51] Waqas Sultani, Chen Chen, and Mubarak Shah. Real-world anomaly detection in surveillance videos. In *Proceedings of the IEEE Conference on Computer Vision and Pattern Recognition*, pages 6479–6488, 2018. 1, 2, 3, 4, 5, 6, 7
- [52] Yu Tian, Gabriel Maicas, Leonardo Zorron Cheng Tao Pu, Rajvinder Singh, Johan W Verjans, and Gustavo

- Carneiro. Few-shot anomaly detection for polyp frames from colonoscopy. In *Medical Image Computing and Computer Assisted Intervention—MICCAI 2020: 23rd International Conference, Lima, Peru, October 4–8, 2020, Proceedings, Part VI* 23, pages 274–284. Springer, 2020. 2
- [53] Shashanka Venkataramanan, Kuan-Chuan Peng, Rajat Vikram Singh, and Abhijit Mahalanobis. Attention guided anomaly detection and localization in images. *arXiv preprint arXiv:1911.08616*, 2019. 2
- [54] B. Wan, Y. Fang, X. Xia, and J. Mei. Weakly supervised video anomaly detection via center-guided discriminative learning. In *2020 IEEE International Conference on Multimedia and Expo (ICME)*, pages 1–6, 2020. 3, 6
- [55] Fei Wang, Mengqing Jiang, Chen Qian, Shuo Yang, Cheng Li, Honggang Zhang, Xiaogang Wang, and Xiaoou Tang. Residual attention network for image classification. In *Proceedings of the IEEE conference on computer vision and pattern recognition*, pages 3156–3164, 2017. 3
- [56] Jue Wang and Anoop Cherian. Gods: Generalized one-class discriminative subspaces for anomaly detection. In *Proceedings of the IEEE International Conference on Computer Vision*, pages 8201–8211, 2019. 2, 4, 7
- [57] Jiang Wang, Yang Song, Thomas Leung, Chuck Rosenberg, Jingbin Wang, James Philbin, Bo Chen, and Ying Wu. Learning fine-grained image similarity with deep ranking. In *Proceedings of the IEEE Conference on Computer Vision and Pattern Recognition*, pages 1386–1393, 2014. 2
- [58] Xiaolong Wang, Ross Girshick, Abhinav Gupta, and Kaiming He. Non-local neural networks. In *Proceedings of the IEEE conference on computer vision and pattern recognition*, pages 7794–7803, 2018. 3, 4
- [59] Peng Wu, jing Liu, Yujia Shi, Yujia Sun, Fangtao Shao, Zhaoyang Wu, and Zhiwei Yang. Not only look, but also listen: Learning multimodal violence detection under weak supervision. In *European Conference on Computer Vision (ECCV)*, 2020. 1, 2, 3, 4, 6, 7
- [60] Dan Xu, Elisa Ricci, Yan Yan, Jingkuan Song, and Nicu Sebe. Learning deep representations of appearance and motion for anomalous event detection. *arXiv preprint arXiv:1510.01553*, 2015. 2
- [61] Dan Xu, Rui Song, Xinyu Wu, Nannan Li, Wei Feng, and Huihuan Qian. Video anomaly detection based on a hierarchical activity discovery within spatio-temporal contexts. *Neurocomputing*, 143:144–152, 2014. 3
- [62] Kelvin Xu, Jimmy Ba, Ryan Kiros, Kyunghyun Cho, Aaron Courville, Ruslan Salakhudinov, Rich Zemel, and Yoshua Bengio. Show, attend and tell: Neural image caption generation with visual attention. In *International conference on machine learning*, pages 2048–2057, 2015. 3
- [63] Zichao Yang, Xiaodong He, Jianfeng Gao, Li Deng, and Alex Smola. Stacked attention networks for image question answering. In *Proceedings of the IEEE conference on computer vision and pattern recognition*, pages 21–29, 2016. 3
- [64] Fisher Yu and Vladlen Koltun. Multi-scale context aggregation by dilated convolutions. *arXiv preprint arXiv:1511.07122*, 2015. 2, 4
- [65] Guang Yu, Siqi Wang, Zhiping Cai, En Zhu, Chuanfu Xu, Jianping Yin, and Marius Kloft. Cloze test helps: Effective video anomaly detection via learning to complete video events. *arXiv preprint arXiv:2008.11988*, 2020. 6
- [66] J. Zhang, L. Qing, and J. Miao. Temporal convolutional network with complementary inner bag loss for weakly supervised anomaly detection. In *2019 IEEE International Conference on Image Processing (ICIP)*, pages 4030–4034, 2019. 2, 3, 6, 7
- [67] Tianzhu Zhang, Hanqing Lu, and Stan Z Li. Learning semantic scene models by object classification and trajectory clustering. In *2009 IEEE conference on computer vision and pattern recognition*, pages 1940–1947. IEEE, 2009. 2
- [68] Ying Zhang, Huchuan Lu, Lihe Zhang, Xiang Ruan, and Shun Sakai. Video anomaly detection based on locality sensitive hashing filters. *Pattern Recognition*, 59:302–311, 2016. 1
- [69] Hengshuang Zhao, Jiaya Jia, and Vladlen Koltun. Exploring self-attention for image recognition. In *Proceedings of the IEEE/CVF Conference on Computer Vision and Pattern Recognition*, pages 10076–10085, 2020. 2, 3, 4
- [70] Jia-Xing Zhong, Nannan Li, Weijie Kong, Shan Liu, Thomas H Li, and Ge Li. Graph convolutional label noise cleaner: Train a plug-and-play action classifier for anomaly detection. In *Proceedings of the IEEE Conference on Computer Vision and Pattern Recognition*, pages 1237–1246, 2019. 1, 2, 3, 4, 6, 7
- [71] Kang Zhou, Yuting Xiao, Jianlong Yang, Jun Cheng, Wen Liu, Weixin Luo, Zaiwang Gu, Jiang Liu, and Shenghua Gao. Encoding structure-texture relation with p-net for anomaly detection in retinal images. *arXiv preprint arXiv:2008.03632*, 2020. 2
- [72] Yi Zhu and Shawn Newsam. Motion-aware feature for improved video anomaly detection. *arXiv preprint arXiv:1907.10211*, 2019. 2, 3, 7
- [73] Bo Zong, Qi Song, Martin Renqiang Min, Wei Cheng, Cristian Lumezanu, Daeki Cho, and Haifeng Chen. Deep autoencoding gaussian mixture model for unsupervised anomaly detection. In *International Conference on Learning Representations*, 2018. 2